Long-term efficiency for reducing entanglements of nascent polyethylene by a polystyrene modified Ziegler-Natta catalyst

Yanjie Wu[1], Yu Cao[1], Xin Tang[1], Ning Wang[1], Siegfried Stapf[2], Carlos Mattea[2], Wei Li[*1]

[1]Ningbo Key Laboratory of Specialty Polymers, School of Material Science and Chemical Engineering, Ningbo University, Ningbo 315211, P.R. China

[2]Fachgebiet Technische Physik II/Polymerphysik, Institut für Physik, TU llmenau, 98684 llmenau, Postfach 10 05 65, Germany

To whom should be correspondence: Wei Li: liwei@nbu.edu.cn

Abstract

Chains entanglement plays a significant role in the mechanical and processable performance of the nascent ultrahigh molecular weight polyethylene (UHMWPE). In this work, the weakly entangled UHMWPE was synthesized by a Ziegler-Natta catalyst, where the titanium tetrachloride was anchored on the polystyrene (PS) modified silica. The PS chains were incorporated into silica pores through the *in-situ* free-radical polymerization of styrene. This incorporated PS was proved to be coated on the surface of pore walls. The self-diffusion coefficients and crystallization of probed molecules were investigated by the pulsed field gradient NMR and thermoporosimetry to address the swollen behavior of the coated PS phase. This swollen PS formed numerous horizontal isolators to compartmentalize the active sites and adjacent chains. The ubiquitous isolators effectively limited the formation of chains overlaps during the polymerization, showing a long-term efficiency to reduce the entanglements of nascent UHMWPE with an exceptional activity (even at 4 h of polymerization). The toughness/stiffness/strength balance of weakly entangled UHMWPE was significantly improved, since the enhanced chain diffusion rate limited the formation of forming defects. Thus, the simultaneously increased impact resistance (+ 53.5 %), Young's modulus (+ 188.2 %) and tensile strength (+ 44.2%) were achieved, compared with those of entangled UHMWPE.

KEYWORDS: Heterogeneous catalysis; Entanglement; Confined polymerization; High-performance polyethylene; mechanical property

1 INTRODUCTION

Ultrahigh molecular weight polyethylene (UHMWPE), with the molecular weight larger than one million g/mol, has been widely used in the military, commercial and medical fields owing to its good mechanical properties, chemical stability and biocompatibility.[1] These excellent properties are attributed to its enormous molecular mass and inert hydrocarbon composition. [2,3] However, the enormous molecular mass inevitably induces the formation of large number of entanglements, which makes the UHMWPE hard to be processed by the conventional methods and limits the mechanical, thermal and electrical properties. [4]

Reduced the entanglement density of nascent UHMWPE endows less confined topology structure, which has been evidenced to retard the formation of defects [5], improve the chain diffusion [6,7], and enhance the transfer of phonon and electron [8,9]. For example, a weakly entangled UHMWPE was synthesized by Rastogi[10], where the fused stripes were more easily to be oriented and successfully biaxial stretched to 188 times. The highly oriented stripe facilitated the transfer of phonons, enhancing the thermal conductivity (i.e., 18.4 W/m K) even comparable to stainless steel [8].

Generally, enlarging the distance of active sites with the assistance of accelerated chain crystallization rate had been proved to be an effective method for reducing the entanglement density of nascent polyethylene [4,11]. For instance, Rastogi et al synthesized the weakly entangled UHMWPE by ethylene polymerization below 30 °C, where the FI catalyst was dispersed in a large volume of toluene. The low temperature significantly enhanced the chain crystallization rate which was even

higher than that of chain propagation rate. This made the propagated chains to be crystallized as soon as they were growing up, reducing the formation of entanglements. [4,12] Mecking et al. synthesized a branch-free polyethylene according to the compartmentalization of active sites with the assistance of surfactant at 10 °C. This synthesized polyethylene represented ideal polymer crystals, showing the exceptional crystallinity χ(DSC) up to 93%.[13,14] Such homogeneous strategy is able to synthesize the less entangled UHMWPE with a much higher molecular weight by the extension of polymerization time, since the fast decay of catalytic activity hinders the formation of entanglement. [12] However, the homogenous catalyst combined with the low temperature polymerization is hard to be realized in industry, due to the difficulty of heat transfer, low catalytic activity, and out of control on the particle morphology. [15,16]

Heterogeneous catalyst is most widely used in industry thanks to its ability in preventing the fouling, directing the particle morphology and elongating the catalytic life, which is endowed by the hierarchical porous structure, and the appropriated stiffness and morphology of support particles. [17,18] Generally, the active species are gradually activated along with the fragmentation of support and the diffusion of reactants, accelerating the propagation of chains and increasing the molecular weight[17,19]. However, the randomly distributed active sites enviably enhances the formation of entanglement, which is further deteriorated due to the formation of more active sites at the long reaction time. [4,20] It shall be mentioned that the chain crystallization rate is decreased in exponential as the increment of temperature. [21] The

UHMWPE synthesized at the industrial temperature (above 60 °C) is enviably of highly entangled. [4,22] A heterogeneous catalysis had been proposed by our group where the POSS blocks were incorporated into the porous silica by impregnation. [23,24] These POSS blocks, with the size of 40-100 nm, were proved to be deactivated toward ethylene polymerization, severing as the horizontal isolators to separate the propagated chains. As a result, the weakly entangled UHMWPE was synthesized above 60 °C with an exceptional activity. However, this POSS blocks were not able to diffuse into the pores with small size, out of controlling on the chain entanglement. The active sites dispersed in this small pores were evidenced to be activated at the long polymerization time due to the limitation of reactant diffusion. As a result, the entanglements of synthesized polymers dramatically increased as the polymerization went on, although an elevated molecular weight was achieved. [20,23] So far, it is still a challenge to handle the contradiction between the high molecular weight and less entangled state in the heterogeneous catalyst, especially at a long polymerization time, forwardly requiring a long-term efficiency to reduce the entanglement density of nascent polyethylene during the polymerization.

With the explicit aim to conquer the blind area of block diffusion, we have for the first time to employ styrene monomer pre-impregnated into the pores of matrix. This impregnated monomer, after thermally induced polymerization, is able to synthesize the inert polymer blocks (i.e., polystyrene) inside each pore. Our proposed method is that after the swollen of polystyrene block inside the confined pores, its steric hindrance effect thus serves to (*i*) blocking the nearby positions for anchoring

$TiCl_4$ catalytic molecules and (*ii*) isolating the propagated chains. The efficiency for reducing the entanglements is anticipated to be long lasting during the polymerization.

2. MATERIALS AND METHODS

2.1. Materials. Porous SiO_2 was supplied by W.R. Grace (USA) (Grade 955, average pore diameter=22.6 nm). The titanium (IV) chloride ($TiCl_4$, 99.9 wt%) was purchased from Aladdin (USA). Styrene, a,a'-azoisobutyronitrile (AIBN), triethylaluminum (1 M solution in *n*-heptane) and dichloromethane were supplied by J&K Company (Shanghai, P.R. China). Styrene were depurated on an alumina column to remove the polymerization inhibitors. Di-*n*-butylmagnesium (0.5 M solution in *n*-heptane) was purchased from Acros Organics (Beijing, P.R. China). Polymerization-grade ethylene was supplied by Feldt Industrial Gas Co., Ltd (Ningbo, P.R. China). High purity nitrogen was purchased from Ningbo Fangxin Refining Plant. All gases must be treated by gas refining column (Dalian Shengmai Chemical Co., Ltd.) before using. *n*-heptane was purchased from Ningbo Chemical Reagents Co., China. Dichloromethane and *n*-heptane were distilled over sodium/diphenyl ketone prior to use. All manipulations of experimental parts were conducted under the protection of high purity nitrogen, which was conducted by standard Schlenk techniques or in a glovebox.

2.2. Catalyst Preparation

Preparation of polystyrene modified support. 10 g of SiO_2 was activated at 600 °C for 8 h in vacuum state. Meanwhile, 0.9 ml of styrene monomer and 0.04 g (4% effective vinyl group content) of a, a'-azoisobutyronitrile (AIBN) was stirred with 10

ml of dichloromethane at 25 °C for half an hour, achieving styrene/dichloromethane solution. Then, 2.0 g of the activated SiO_2 was mixed with styrene/dichloromethane solution in another Schlenk flask at room temperature for 24 h, sufficiently impregnating styrene monomer into the pores of SiO_2. The mixture was carried on the cycle of freeze-vacuum-thaw to detach dichloromethane from pores of SiO_2. Subsequently, the temperature programmed polymerization process (i.e, 80 °C for 2 h and 110°C for 4 h) was conducted to polymerize the styrene inside the pores. The obtained solids were washed three times with 20 ml of dichloromethane to remove the unreacted styrene, AIBN and free polystyrene. Finally, the solid particles were dried under the vacuum, achieving the PS modified supports (i.e, SiO_2/X%PS, where X% =0, 2, 4 and 6% represented the actual loading of PS).

Catalyst Immobilization. 1.0 g of SiO_2/X%PS was mixed with 6.0 ml of di-*n*-butylmagnesium under stirring at 60 °C for 4 h. The excessive butylmagnesium was removed by washing with 30 ml of *n*-heptane three times. 1 ml of titanium (IV) chloride was dissolved in 10 ml of *n*-heptane at 60 °C. Then, the diluted $TiCl_4$ was injected into the suspension, which was stirred for another 4 h at 60 °C. The solid particles were washed with *n*-heptane three times to remove the unloaded $TiCl_4$. These particles were dried at 60 °C under vacuum to yield reddish brown particles. The catalyst with different PS contents were carried out following the same method, which was named as Cat-SiO_2/X%PS (X=0, 2, 4, 6).

2.3. Ethylene polymerization

Ethylene polymerization was conducted in a Büchi stainless steel autoclave

reactor (1.0 L) equipped with the high-speed agitator. The reactor was heated to 90 °C under vacuum for at least 4 h, and was repeatedly pressurized with nitrogen three times. After that, 350 ml of *n*-heptane was injected into the reactor. TEA ([Al]/[Ti]=100) was introduced into reactor at the same time. The polymerization temperature was set at 70 °C, which was further conducted at 10 bar of ethylene and 500 rpm. The synthesized polyethylene (named as PE-SiO_2/X%PS, X=0,2,4,6) was washed with acidified ethanol for three times and dried for 48 h at 60 °C in vacuum.

2.4. Characterization

Thermal Gravimetric Analyses (TGA SDT 2960 Simultaneous) was conducted to trace the weight loss of the support, reflecting the content of polystyrene in the support. The sample (about 5-10 mg) was heated under nitrogen flow (200 ml·min^{-1}), from 25 °C to 800 °C with a heating rate of 10 °C·min^{-1}.

N_2 adsorption and desorption experiments was carried out on ASAP 2020 instrument (Micromeritics, U.S.A.) at 77 K. The surface area, the average pore size and cumulative volume of pores were calculated by the BET method and the BJH method, respectively.

The X-ray photoelectron spectroscopy (XPS) (AXIS ULTRA DLD), equipped with Al-K_α X-ray source (1486.3 eV), was carried out on the surface element analysis of Cat-SiO_2/0%PS and Cat-SiO_2/6%PS. The C *1s* peak (284.8 eV) was employed to correct the position of other elemental peaks. The Ti (IV) 2*p* spectrum had two different peaks (458.6 and 464.3 eV) which represented to the resonance of Ti $2p_{3/2}$ and Ti $2p_{1/2}$, respectively.

The self-diffusion coefficients of the polystyrene in the pores was analyzed by NMR diffusion measurements (Bruker Avance III NMR spectrometer, 7 T), where *n*-heptane was selected as the probe molecules. The supports (about 0.5 g) were dispersed in this probe liquid (about 1.5 ml) at least for 72 h in a 5 mm of NMR tube. In this way, a thermally stable state of the swollen polystyrene was achieved in the *n*-heptane. The self-diffusion coefficients of probe liquid in the bulk state and support were acquired with the pulsed gradient stimulate echo (PGSTE) sequence. The diffusion time (Δ) was set as 20 ms. 32 scans were acquired at each step. A couple of equal strength magnetic field gradient pulses (g) were shifted 16 steps in 1.0 ms. The signal intensity was attenuated to a specific intensity of stimulated echo signal ($I(g)$) after a sequence. [25,26] The stimulated echo signal intensity curves were achieved by setting different magnetic field gradient pulses values. The signal intensity attenuated to:

$$I(g) = I(0)\exp(-((\Delta-\delta/3)\gamma^2 g^2 \delta^2)D) \qquad Eq.1$$

In this equation, γ referred to the magnetic spin ratio of the atomic nucleus. δ referred to the width of the gradient pulses. The time interval between the two gradient pulses is represented by Δ. The self-diffusion coefficient (D) of the *n*-heptane was acquired by fitting *Eq.1*.

To further understand the swollen behavior of polystyrene inside the pores, the pore size distribution of support, after impregnated in the cyclohexane, was measured by thermoporosimetry method using the TPM-DSC (Mettler Toledo Apparatus DSC 822° equipped with a liquid nitrogen cooling system, where the working temperature

was between -100 and 400 °C). This method was mainly depended on the crystallization behavior of probe molecules (cyclohexane) inside the pores, where the polystyrene chains correspondingly showed swollen behavior.[27] All the testing processes were internally calibrated for temperature to ensure the accuracy of the results before experiment. Supports (about 4.0 mg) was put in an aluminum pan, followed by heating at 150 °C for 30 min to purify the pores of powder. According to the Gibbs-Thomson equation, the shift of melting point was inversely proportional to the pore radius, which provided the reference to calculate the pore size distribution.[27,28]

The melting temperature and crystallinity of nascent polyethylene were carried on the differential scanning calorimetry (DSC, PerkinElmer Corp., USA). The polyethylene (about 5-8 mg) was tested followed a heating, cooling and re-heating program, ranging from 50 to 160 °C with a 10 °C/min of rate. The melting temperature was obtained from the peak of melting curve. The crystallinity was obtained by dividing the fusion enthalpy to that of the perfectly crystalline polyethylene (i.e., 289 J/g).

The viscosity average molecular weight of nascent polyethylene was determined by ASTM D4020-2011 using Ubbelohde viscometer. Decahydronaphthaline was chosen as the solvent to prepare the standard solution (0.040 g/ (100 ml)) in a silicone oil bath at 150 °C. This standard solution was diluted to different concentrations (0.008, 0.016, 0.024, 0.032, 0.040 g/ (100ml)). The efflux time (t_0 and t) of solvent decalin was measured by Ubbelohde viscometer in a silicone oil bath at 135 °C. The

intrinsic viscosity of nascent polyethylene was obtained by the extrapolation method. The viscosity average molecular weight (M_η) of nascent polyethylene was calculated by mark Houwink equation.

The weight-average molar mass (M_w) and molecular weight distribution (PDI) of the polymer were obtained by high-temperature gel permeation chromatography, where 1,2,4-trichlorobenzene was selected as the solvent with a flow rate of 1 ml/min. The measured temperature was maintained at 150 °C. The narrowly distributed polystyrene ranging from 1,000 to 14,000,000 g/mol was used to make the standard curve. [22-24]

The amount of titanium in the catalyst was measured through the method of hydrogen peroxide colorimetric, which was conducted on an ultraviolet-visible instrument spectrophotometer (TU1901, Persea, China). [23] The powder was immersed and stirred in the dilute sulfuric acid (25 ml, 1 M) for at least 8 h. Then, the hydrogen peroxide solution (2.0 ml) was added in the solution. Titanium potassium oxalate standards were used to set standard curves of titanium content in the dilute solution ($Abs_{Ti} = 14.3\ C_{Ti} - 0.00133$, $R^2 = 0.99997$).

The morphology of supports and nascent polyethylene were investigated by a field emission scan electron microscope (SEM, Hitachi S-4700, Japan). The SEM testing voltage was 5.0 kV. The samples were coated with platinum at least 30 s to improve the conductivity.

Nascent polyethylene particles were made into dumbbell (gauge length 20 mm) for the tensile test. Tensile strength, Young's modulus and break elongation were

determined based on GB/T 1040.2-2006 using the CMT 4204 electronic universal testing machine. Notched splines (80×10×4 mm) were made for conducting the falling dart impact tests, which was carried out according to GB/T 1843-2008 using the ZBC 1750 plastic pendulum impact testing machine. The tensile and impact tests were repeated at least 5 times for each spline.

The entanglement density of nascent ethylene was investigated by the rheological studies through a strain-controlled rheometer (HAAKE MARS III instrument). [4] Antioxidant (Irganox 1010, 0.6 wt%) was added in the nascent polyethylene to inhabit the degradation during the test. Then, a round plate (20 mm diameter, 2 mm thickness) was prepared under the pressure of 20 MPa for 30 min at 130 °C. Dynamic time sweep test was characterized at the 10 rad/s of frequency and 0.5% of strain in the linear viscoelastic regime, tracing the entanglement of nascent polyethylene. [4,23] This work was devoted to determine the inter-diffusion process of long chains during the formation of entanglements, which addressed the chain dynamics of polyethylene chains. The self-diffusion coefficient (D_{rep}) of the polyethylene was calculated based on Doi-Edwards theory.

$$D_{rep} = \frac{k_B T N e^2}{3 \xi N^2 b^2} \qquad Eq.2$$

In *Eq2*, N was the number of segments per chain and b was the effective bond length. N_e is the number of segments (Kuhn segments) corresponding to the entanglement. For $N > N_e$ you will have "entangled dynamics". T is the temperature; k_B is Boltzmann

constant. ξ is the friction coefficient. The related expressions between the storage modulus *G'* and D_{rep} were proposed by Qiu and Bousmina from Boltzmann's integral as follows Eq3: [29,30]

$$\left[G'(\omega)\right]^2=\left(\frac{8G_N^0}{\pi^2}\right)^2\frac{1}{1+\left(\frac{3\pi^2 D_{rep}}{\omega N b^2}\right)^2} \qquad Eq3$$

Where, the angular velocity (ω) was set as 10 rad/s. The G_N^0 was the plateau modulus of UHMWPE. [4] Substituting *Eq.3* into *Eq.2*, the relationship between the storage modulus *G'(ω)* and self-diffusion coefficients D_{rep} was expressed as follows Eq4:

$$D_{rep}=\frac{N b^2 \omega}{3\pi^2}\left[\left(\frac{8G_N^0}{\pi^2 G'(\omega)}\right)^2-1\right]^{1/2} \qquad Eq.4$$

3. RESULTS AND DISCUSSION

3.1. Microstructure of the PS filled SiO_2 support

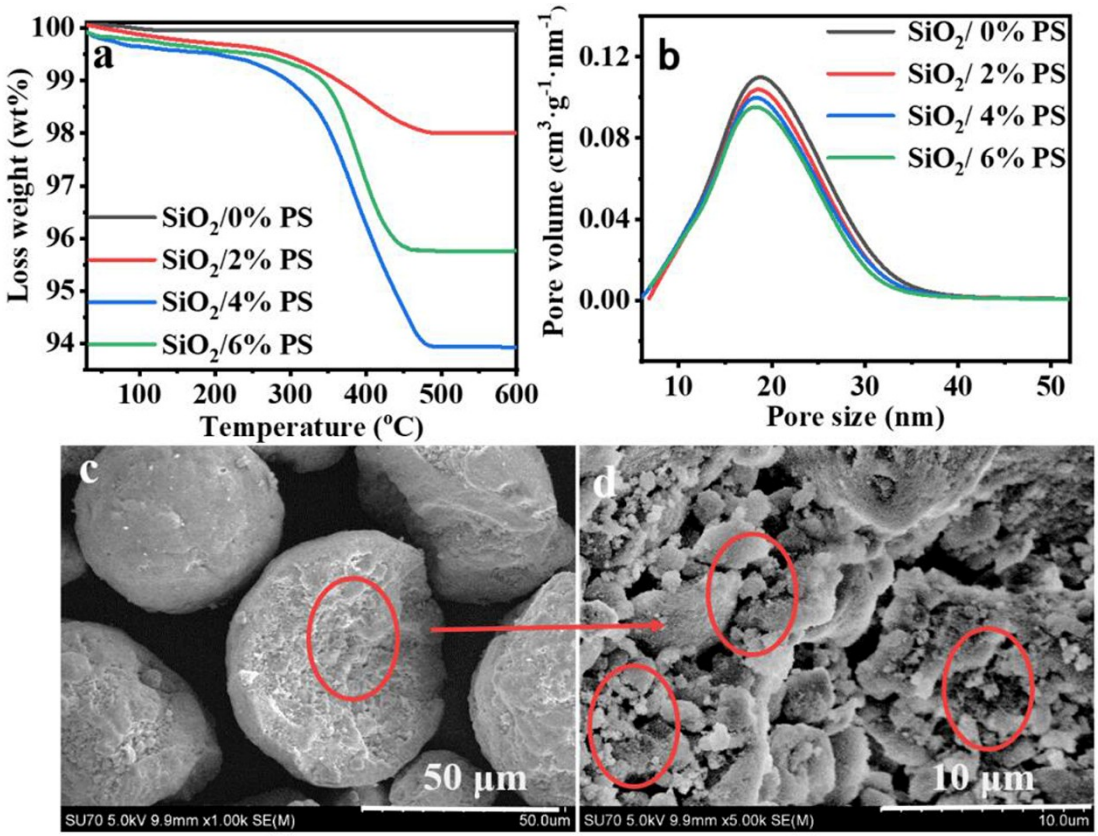

Figure 1. Microstructure of the support. a. The loss weight curves of supports determined by the TGA; b. The pore size distribution of SiO_2 and SiO_2/X%PS carried on the Brunauer-Emmett-Teller (BET) method; c-d. Typical SEM morphology of the Cat-SiO_2/6%PS were observed in the different scales.

The microstructure of the support is investigated by several techniques (See in Figure 1). Weight loss temperature of support at around 240 °C is correspond to the loss point of polystyrene. [31] The SiO_2/PS composite finally turns to be black, indicating the carbonization of PS. These further evidences that the impregnated styrene monomer is able to be *in-situ* polymerized in the silica pores. This filling is further evidenced by the BET results, where the pore size distribution shows a

downward shift even in the pores less than 10 nm (**Figure 1b**). Here, the hysteresis loop exhibiting sharp change (around P/P_0=0.9) is a feature of mesopore with the open cylindrical geometry (**Figure S1**). The narrow adsorption-desorption hysteresis loop is maintained after the loading of polystyrene, which further implies that the polystyrene is uniformly deposited in the pore of silica without blockage [32]. In addition, the average pore size, pore volume and surface area of the SiO_2/X%PS are slightly decreased with the increment of PS loading, further proving the successful impregnation of PS (**See Table S1**). The result of SEM morphology (**Figure 1c,d**) also shows that the polystyrene is incorporated in the pores without blocking the channel of silica.

The surface Mg and Ti elements of the PS modified catalyst are examined by XPS analysis (**Figure 2a,b**). The binding energy of Mg 2*p* for cat-SiO_2/6%PS and cat-SiO_2/0%PS are the same (i.e., 51.1 eV), indicating the same chemical environment of Mg atoms. With the immobilization of $TiCl_4$, the similar value of the full wave at half-maximum (FWHM) (i.e., 1.8 eV) and BE of Ti(IV) $2p_{3/2}$ (i.e., 458.9 eV) are shown in the PS-modified and PS-free catalyst, indicating that the incorporated PS shows no effect on the electric environment of Ti atoms (see **Figure 2b** and **Figure S2**). It is reasonable to deduce the inert PS phase present no influence on the catalytic feature of active species.

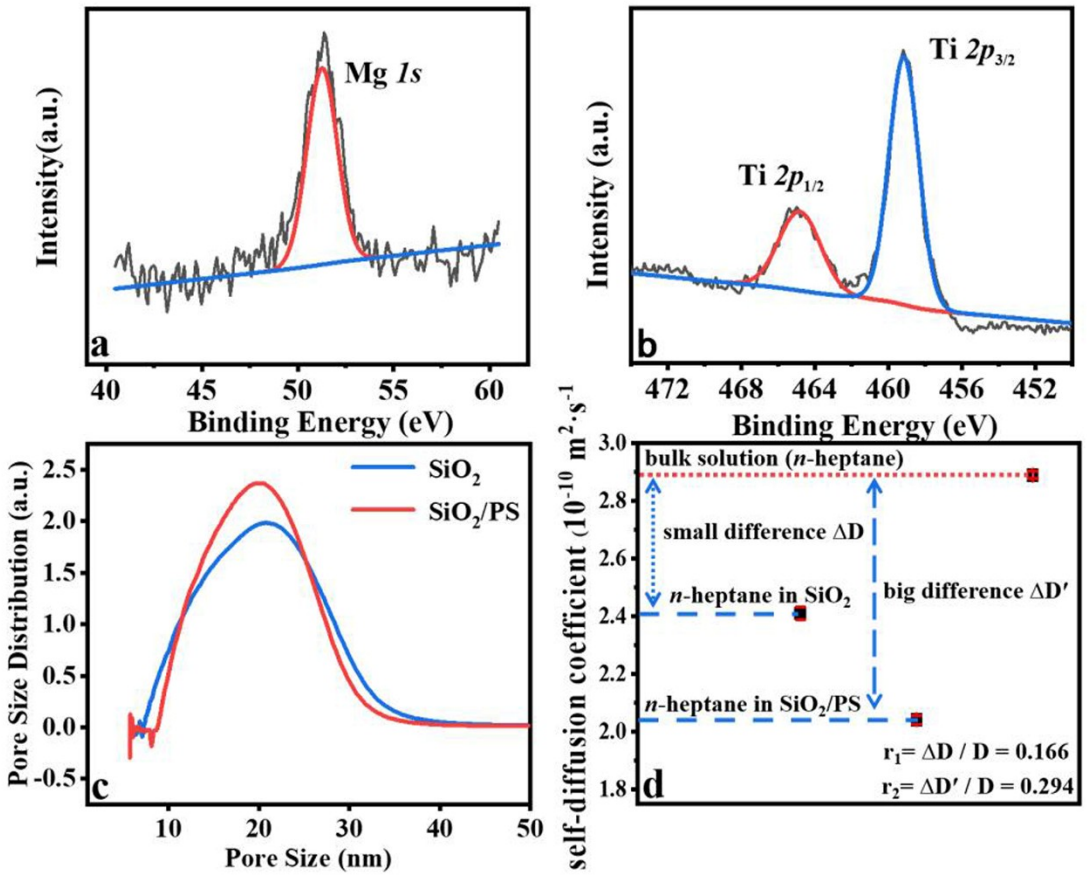

Figure 2. a. Typical XPS spectrum over Mg *1s* of cat-SiO_2/6%PS; b. XPS spectrum over Ti *2p* of cat-SiO_2/6%PS; c. The pore size distribution of SiO_2 and SiO_2/6%PS after immersing in the cyclohexane; d. The self-diffusion coefficient of *n*-heptane in SiO_2 and SiO_2/6%PS.

The swelling behavior of polystyrene confined in the silica pores is investigated by TPM-DSC and PFG-NMR, where the support is pre-impregnated in the cyclohexane. Compared with the SiO_2, the pore of SiO_2/6%PS is significantly shrinking, indicating that the polystyrene chains confined in the pores of silica are swelling (**Figure 2c**). The self-diffusion coefficients of *n*-heptane in the matrix of SiO_2 and SiO_2/6%PS are examined by the pulsed field gradient (PFG) NMR. The self-

diffusion coefficients of *n*-heptane inside the pores are calculated and shown in **Figure 2d**, where a much smaller value is found in the PS modified silica. This corresponds to the results of the TPM-DSC that the swollen PS phase decreases the pore size of silica, confining the constrained dynamics of probe molecules. [26,27]

3.2. Ethylene Polymerization Results

The ethylene polymerization results are shown in **Table 1**, where the catalytic activity is increased upon the incorporation of PS reaching to the maximum in the cat-SiO_2/4%PS (i.e, 3.10×10^6 gPE·mol[Ti] $^{-1}$·h^{-1}). The incorporated PS does not endow the notable transfer resistance to the monomer, since no retardation of ethylene flow is shown during the polymerization.[33] All the catalyst shows the similar time-dependent polymerization kinetics, indicating the same polymerization mechanism (See **Figure S3**). In addition, the activity should be reduced with the incorporation of PS, because the decreased pore size and surface ratio could limit the diffusion of small molecules [33]. However, this enhanced activity may be attributed to the isolated effect of PS phase, since the inert PS phase presents no location for anchoring the active species. The reduction of catalytic activity in the cat-SiO_2/6%PS is due to the blocking of the channels by the excessively filled PS. [24] This is further evidenced from the molecular weight of the synthesized polymers (See the GPC curves in **Figure 4**). All the synthesized polymer had a molecular weight (M_η) larger than 1.5 million g/mol, demonstrating the synthesis of UHMWPE. The molecular weight is exceptionally increased with the incorporation of PS. However, a slight variance of molecular

weight is shown upon the increment of PS loading. This indicates that the isolated effect of PS phase is able to hinder the bimetallic deactivation, rising the molecular weight of the synthesized polymers. With the extension of polymerization time, a much higher molecular weight of the synthesized UHMWPE is achieved (i.e., 3.2 $\times 10^6$ g/mol). The synthesized polymer shows an increment on the melting point and crystallinity in the PS modified system, indicating the increased lamella size of the nascent polymers.

Table 1. The results of ethylene polymerization by varying the content of PS. [a]

Samples	Yield (g)	Activity [b]	T_m^1 (°C)	T_m^2 (°C)	X_c^1 (%)	X_c^2 (%)	M_η [c]	M_w [d]
PE-SiO_2/0%PS	64.9	2.16	142.3	137.8	64.9	50.4	155.3	119.2
PE-SiO_2/2%PS	72.3	2.41	144.2	137.5	65.5	46.5	246.2	119.8
PE-SiO_2/4%PS	93.1	3.10	144.2	138.8	66.5	47.2	262.6	125.0
PE-SiO_2/6%PS	74.3	2.47	143.1	137.5	67.2	48.4	271.6	127.1
PE-SiO_2/6%PS-0.5h	25.8	2.06	141.7	137.6	65.2	52.6	176.5	103.5
PE-SiO_2/6%PS-1h	74.3	2.47	143.1	137.5	67.2	48.4	271.6	127.1
PE-SiO_2/6%PS-2h	183.9	3.68	143.1	137.6	68.1	49.5	289.1	137.3
PE-SiO_2/6%PS-4h	188.0	3.13	145.8	138.0	67.5	49.8	324.8	144.8

a. Polymerization condition: $P_{C_2H_4}$ = 7 bar, T = 70 °C, t = 60 min and $n_{catalyst}$ = 30 μmol of $TiCl_4$, cocatalyst TEA, [Al]/[Ti] = 100, 350 ml of *n*-heptane solution;

b. Activity unit is$\times 10^6$ gPE·(molTi·h)$^{-1}$;

c. M_η unit is $\times 10^4$ g·mol^{-1}.

d. M_w unit is $\times 10^4$ g·mol^{-1}.

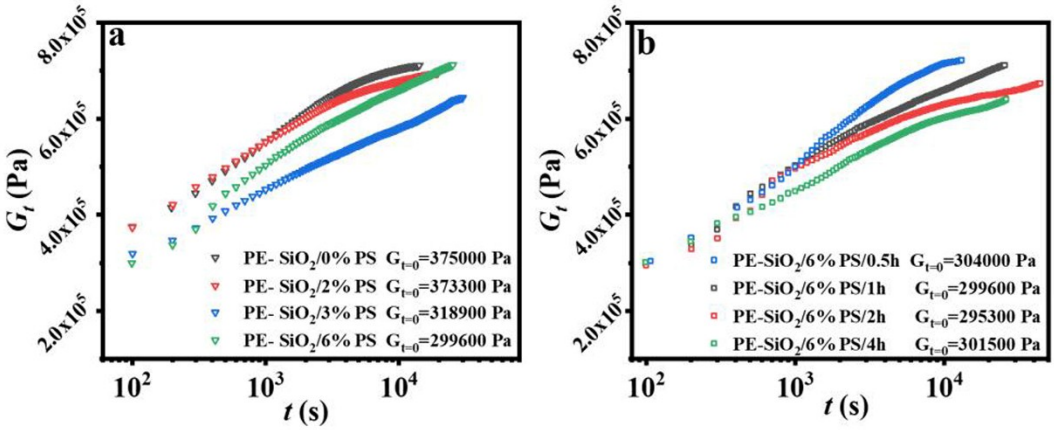

Figure 3. a. Dynamic time sweep test at 160 °C of nascent polyethylene synthesized by varying PS content. b. Dynamic time sweep test at 160 °C of nascent polyethylene synthesized at dynamic time sweep test.

Dynamic time sweep measurements are used to investigate the entanglement density of the nascent polymers (**Figure 3**). At a given time t, G'_t indicates the present entangled state which is inversely proportional to the molecular weight between the entangled points. [4, 23] The initial storage modulus of the synthesized UHMWPE is gradually decreased with the increment of PS loading, indicating the reduced entanglements of the nascent polymer. [23] The polymer synthesized by the cat-SiO_2/6%PS presents a rather low initial storage modulus (i.e., 268200 Pa **Figure 3a**) and takes the longest time (t_m =73150 s) to reach the maximum modulus, demonstrating the most disentangled state. This indicates that the swelling behavior of PS phase endows the compartmentalization of active sites, which is able to hinder the formation of chain overlaps. Interestingly, the initial storage modulus of the nascent polymers synthesized at different time are almost the same, suggesting the entangled

state of nascent polymers is stable (See **Figure 3b**). This demonstrates that the PS phase locating in the pores can steadily endow the compartmentalization of active sites during the polymerization. As a result, the long-term efficiency to reduce the entanglement density of nascent UHMWPE is successfully achieved with the accompaniment of elevating the molecular weight. Moreover, the nascent UHMWPE with a less entangled state shows a much higher melting point and crystallinity which are further lost during the second heating scan due to the formation of entanglement (See the DSC curves in **Figure S5**).

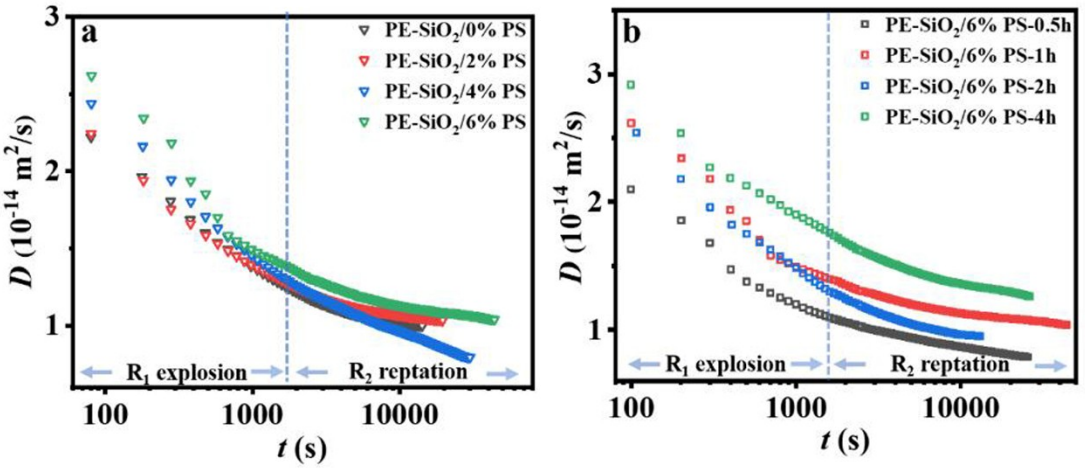

Figure 4. a. Dependence of self-diffusion coefficients on the annealing time. (a) the polymer synthesized by different catalyst; (b) the polymer synthesized at different time.

The chain dynamics of nascent UHMWPE during the thermal annealing are traced according to the evolution of self-diffusion coefficients (See **Figure 4**). Typically, the self-diffusion coefficients are gradually decreased with the increment of annealing time, where two regions are present. The former with the fast decay of self-

diffusion coefficients corresponds to the process of chain explosion on melting, associated with the entanglement formation by fast mixing of polymer chains.[4,12] The latter showing the slow decay of self-diffusion coefficients is the reflection of chain reptation dynamics, where the chain mixing dynamics and space are quite confined.[4,12] After the disentangled molten reaches to the thermodynamics equilibrium, the self-diffusion coefficients become the minimum. Interestingly, the turning point between the R_1 and R_2 region gradually shifts to a much longer time, when the entanglements of nascent UHMWPE are reduced. In particular, the nascent UHMWPE synthesized by the cat-SiO_2/6%PS can stay in the R_1 region more than 1000 s, owing to its most disentangled state. This fast chain dynamic facilitates the chain mixing process, which is favor to the improvement of interfacial fusion. [7,29] However, the entangled UHMWPE will be rapidly transferred to the reptation zone, confining the chain dynamics and limiting the diffusion. [7] Moreover, different chain dynamics are present in the UHMWPE synthesized by the variance of polymerization time, although they have the same initially entangled state (i.e., the same $G'_{t=0}$). The less entangled polymer with a larger molecular weight presents much higher and slower decay of self-coefficients, owing to the enhancement on heterogeneous dispersion of entangled points.[4] In particular, the number of entangled points is proportional to the molecular weight at the thermally dynamic state. A much heterogeneous dispersion of entanglements will be achieved in the nascent disentangled melts with a higher molecular weight.[12]

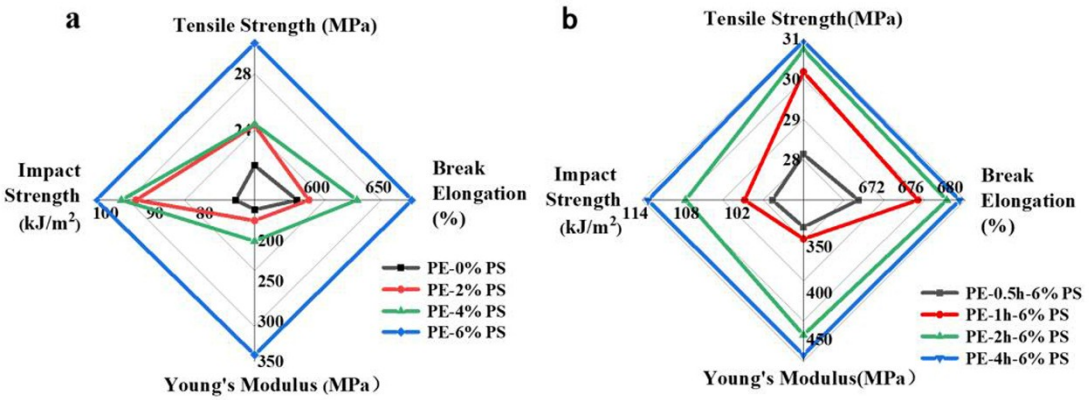

Figure 5. Radar map of mechanical properties for various nascent UHMWPE. a) the polymer synthesized by different catalyst, b) the polymer synthesized by different time.

The mechanical properties of the synthesized polyethylene are shown in **Figure 5**, where the data are list in **Table S2**. The UHMWPE synthesized by the PS modified catalyst presents a significate enhancement on the mechanical properties, where an improved toughness/stiffness/strength balance are achieved (See the stress-strain curves in **Figure S6**). In particular, the UHMWPE with the most disentangled state (i.e. PE-SiO_2/6%PS) shows a simultaneously increased on the impact resistance (+ 38.1 %), Young's modulus (+ 111.1 %), tensile strength (+ 40.6%) and break elongation (+ 15.9 %), compared with those of the entangled UHMWPE (i.e., PE-SiO_2/0%PS). This is evidenced by the large self-diffusion coefficients, where the less entangled polymer shows a pronounced chain dynamic facilitating the diffusion and mixing of polymer chains. [5,7] This is favor to limiting the formation of defects, enhancing the mechanical properties. [5,6] Interestingly, the prolongation of

polymerization time is favorable for elevating the mechanical properties, although the nascent polymer shows a similar disentangled state (see **Figure 5b**). As is shown in the evolution of self-diffusion coefficients, the UHMWPE synthesized at the long time is able to maintain a high value upon the thermal annealing, which improves chain dynamics and limits the defects during the fusion. In addition, the increased molecular weight also contributes to the enhancement of mechanical properties. [34]

4. CONCLUDING REMARKS

In summary, the polystyrene is incorporated into pores of porous silica according to the *in-situ* free-radical polymerization of styrene which is pre-impregnated into the pores. This incorporated PS, after swelling in the *n*-heptane, serves as the isolator to compartmentalize the active sites and adjacent chains, which is able to improve the catalytic activity and reduce the formation of chain entanglement even at long polymerization time at 70 °C. This long-term efficiency for reducing the entanglements endows the probability to synthesize the less entangled UHMWPE with a much higher molecular weight according to the increment of polymerization time. The polymer with a much higher molecular weight and a less entangled state presents such a high chain diffusion coefficients with a slow decay rate, where the transition point between the chain explosion and reptation can be extent even to 3000 s. This enhanced chain dynamics facilitate the chain mixing and diffusion during the thermal fusion, where the toughness/stiffness/strength balance are enhanced. In particular, a simultaneously increased on the impact resistance (114 kJ/m^2, +53.5%), Young's modulus (+80 Mpa, +188.2%), tensile strength (31.4 Mpa, + 44.2%) and

break elongation (696%, +16.6%) are shown in the UHMWPE synthesized by the cat-SiO_2/6%PS.

ACKNOWLEDGMENTS

The research was supported by the General Program of the National Natural Science Foundation of China (Grant No. 21776141), the key Project of Natural Science Foundation of Ningbo (202003N4014) and the Talent Project of Zhejiang Association for Science and Technology under Grant 2018YCGC014.

REFERENCES

1. Patel K, Chikkali SH, Sivaram S. Ultrahigh molecular weight polyethylene: Catalysis, structure, properties, processing and applications. *Prog Polym Sci.* 2020;109:101290.
2. Scott G, Wiles DM. Programmed-Life Plastics from Polyolefins: A New Look at Sustainability. *Biomacromolecules*. 2001;2:615-622.
3. Kurtz SM. UHMWPE biomaterials handbook: ultra high molecular weight polyethylene in total joint replacement and medical devices. New York: Elsevier Academic Press; 2015.
4. Rastogi S, Lippits DR, Peters GWM, Graf R, Yao Y. Spiess HW. Heterogeneity in polymer melts from melting of polymer crystals. *Nat Mater.* 2005;4(8):635-641.
5. Yue Z, Wang N, Cao Y, Li W, Dong CD. Reduced entanglement density of ultra-high molecular weight polyethylene favored by the isolated immobilization on $MgCl_2$ (110) plane. *Ind Eng Chem Res.* 2020;59(8):3351-3358.

6. Zhang H, Zhao SC, Yu X, Xin Z, Ye CL, Li Z, Xia JC. Nascent Particle Sizes and Degrees of Entanglement Are Responsible for the Significant Differences in Impact Strength of Ultrahigh Molecular Weight Polyethylene. *J Polym Sci Pol Phys*. 2019; 57(10):632-641.
7. Deplancke T, Lame O, Rousset F, Seguela R, Vigier G. Mechanisms of Chain Reentanglement during the Sintering of UHMWPE Nascent Powder: Effect of Molecular Weight. *Macromolecules*. 2015;48(15):5328-5338.
8. Ronca S, Igarashi T, Forte G, Rastogi S. Metallic-like thermal conductivity in a lightweight insulator: Solid-state processed Ultra High Molecular Weight Polyethylene tapes and films. *Polymer*. 2017;123:203-210.
9. Liu KS, Ronca S, Andablo-Reyes E, Forte G, Rastogi S. Unique Rheological Response of Ultrahigh Molecular Weight Polyethylenes in the Presence of Reduced Graphene Oxide. *Macromolecules*. 2015;48(1):131-139.
10. Ronca S, Forte G, Tjaden H, Yao YF, Rastogi S. Tailoring molecular structure via nanoparticles for solvent-free processing of ultra-high molecular weight polyethylene composites. *Polymer*. 2012;53(14):2897-2907.
11. Li W, Guan C, Xu J, Mu JS, Gong DR, Chen ZR, Zhou Q. Disentangled UHMWPE/POSS nanocomposites prepared by ethylene in situ polymerization. *Polymer*. 2014;55(7):1792-1798.
12. Pandey A, Champouret Y, Rastogi S. Heterogeneity in the distribution of entanglement density during polymerization in disentangled ultrahigh molecular weight polyethylene. *Macromolecules*. 2011;44(12):4952-4960.

13. Kenyon P, Wörner M, Mecking S. Controlled polymerization in polar solvents to ultrahigh molecular weight polyethylene. *J Am Chem Soc*. 2018;140(21):6685-6689.
14. Osichow A, Rabe C, Vogtt K, Narayanan T, Harnau L, Drechsler M, Ballauff M, Mecking S. Ideal Polyethylene Nanocrystals. *J Am Chem Soc*. 2013;135(31):11645-11650.
15. Stürzel M, Mihan S, Mülhaupt R. From Multisite Polymerization Catalysis to Sustainable Materials and All-Polyolefin Composites. *Chem Rev.* 2016;116(3):1398-1433.
16. Christophe C, Florian A, Chan KW, Matthew PC, Murielle FD, Alexey F, Ilia BM, Victor M, Margherita P, Keith S, Keishi Y, Pavel AZ. Bridging the Gap between Industrial and Well-Defined Supported Catalysts. *Angew Chem Int Ed.* 2018;57(22):6398-6440.
17. McDaniel MP. Influence of Catalyst Porosity on Ethylene Polymerization. ACS Catal. 2011;1(10):1394-1407.
18. Klapper M, Joe D, Nietzel S, Krumpfer JW, Müllen K. Olefin Polymerization with Supported Catalysts as an Exercise in Nanotechnology. *Chem Mater.* 2014;26(1):802-819.
19. McKenna TFL, Martino AD, Weickert G, Soares JBP. Particle Growth During the Polymerisation of Olefins on Supported Catalysts, 1-Nascent Polymer Structures. *Macromol React Eng.* 2010;4(1):40-64.
20. Hui L, Yue Z, Tang HQ, Chen T, Li W. Influence of the Fragmentation of POSS-

Modified Heterogeneous Catalyst on the Formation of Chain Entanglements. *Ind Eng Chem Res.* 2018;57(29):9400-9406.

21. Ungar G, Stejny J, Keller A, Bidd I, Whiting MC. The crystallization of ultralong normal paraffins: the onset of chain folding. *Science.* 1985;229(4711):386-389.
22. Li W, Hui L, Xue B, Dong XD, Chen YM, Hou LX, Jiang BB, Wang JD, Yang YR. Facile high-temperature synthesis of weakly entangled polyethylene using a highly activated ziegler-natta catalyst. *J Catal.* 2018;360:145-151.
23. Chen YM, Liang P, Yue Z, Li W, Dong CD, Jiang BB, Wang JD, Yang YR. Entanglement formation mechanism in the POSS modified heterogeneous Ziegler-Natta Catalysts. *Macromolecules.* 2019;52(20):7593-7602.
24. Li W, Yang HQ, Zhang JJ, Mu JS, Gong DR, Wang XD. Immobilization of isolated FI catalyst on polyhedral oligomeric silsesquioxane-functionalized silica for the synthesis of weakly entangled polyethylene. *Chem Commun.* 2016;52(74):11092-11095.
25. Sørland GH, Hafskjold B, Herstad O. A Stimulated-Echo Method for Diffusion Measurements in Heterogeneous Media Using Pulsed Field Gradients. *J Magn Reson.* 1997;124(1):172-176.
26. Jobic H, Paoli H, Méthivier A, Ehlers G, Kärger J, Krause C. Diffusion of *n*-hexane in 5A zeolite studied by the neutron spin-echo and pulsed-field gradient NMR techniques. *Micropro Mesopor Mat.* 2003;59(2-3):113-121.
27. Jackson CL, McKenna GB. The melting behavior of organic materials confined in porous solids. *J Chem Phys.* 1990;93(12):9002-9011.

28. Petrov OV, Furó I. NMR cryoporometry: Principles, applications and potential. *Prog Nucl Magn Reson Spectrosc*. 2009, 2(54): 97-122.
29. Zhao R, Macosko CW. Polymer-polymer mutual diffusion via rheology of coextruded multilayers. *AICHE J*. 2007;53(4):978-985.
30. Zhang HG, Lamnawar K, Maazouz A. Rheological modeling of the diffusion process and the interphase of symmetrical bilayers based on PVDF and PMMA with varying molecular weights. *Rheol Acta.* 2012;51(8):691-711.
31. Wight AP, Davis ME. Design and Preparation of Organic-Inorganic Hybrid Catalysts. *Chem Rev.* 2002;102(10):3589-3614.
32. Choi M, Kleitz F, Liu D, Lee HY, Ahn WS, Ryoo R. Controlled Polymerization in Mesoporous Silica toward the Design of Organic-Inorganic Composite Nanoporous Materials. *J Am Chem Soc.* 2005;127(6):1924-1932.
33. Li W, Jiang BB, Wang JD, Yang YR. Organic/inorganic support for immobilizing (n-BuCp)$_2$ZrCl$_2$/TiCl$_3$ hybrid catalyst for use in the preparation of polymer blends *Polym Int.* 2011;60(4):676-684.
34. Li Z, Zhang W, Feng LY, Shen XT, Mai YY. Role of the amorphous morphology in physical properties of ultrahigh molecular weight polyethylene. *Polym Plast Technol Eng.* 2014;53(11):1194-1204.

SUPPORTING INFORMATION

Additional supporting information may be found online in the Supporting Information section at the end of this article.